

# Inference of Polygenic Factors Associated with Breast Cancer: Gene Interaction Networks from Discrete Data Utilizing Poisson Multivariate Mutual Information

Jeremie Fish,<sup>1,2</sup> Daqing Hou,<sup>1,2</sup> Jie Sun,<sup>2</sup> and Erik Boltt<sup>1,2</sup>

<sup>1</sup>*Department of Electrical and Computer Engineering Clarkson University*

<sup>2</sup>*Clarkson Center for Complex Systems Science\**

(Dated: February 6, 2020)

In this work we introduce a new methodology to infer from gene expression data the complex interactions associated with polygenic diseases that remain a major frontier in understanding factors in human health. In many cases disease may be related to the covariance of several genes, rather than simply the variance of a single gene, making network inference crucial to the development of potential treatments. Specifically we investigate the network of factors and associations involved in developing breast cancer from gene expression data. Our approach is information theoretic, but a major obstacle has been the discrete nature of such data that is well described as a multi-variate Poisson process. In fact despite that mutual information is generally a well regarded approach for developing networks of association in data science of complex systems across many disciplines, until now a good method to accurately and efficiently compute entropies from such processes as been lacking. Nonparametric methods such as the popular k-nearest neighbors (KNN) methods are slow converging and thus require unrealistic amounts of data. We will use the causation entropy (CSE) principle, together with the associated greedy search algorithm optimal CSE (oCSE) as a network inference method to deduce the actual structure, with our multi-variate Poisson estimator developed here as the core computational engine. We show that the Poisson version of oCSE outperforms both the Kraskov-Stögbauer-Grassberger (KSG) oCSE method (which is a KNN method for estimating the entropy) and the Gaussian oCSE method on synthetic data. We present the results for a breast cancer gene expression data set.

## I. INTRODUCTION

It is well understood that many diseases can be prescribed to the variation of the expression of a single gene [1–3], e.g., famously such as sickle cell disease and cystic fibrosis. However it remains a difficult health problem to explain and to infer complex interactions and associations when many genes may be involved in common and even deadly disease. Such diseases are called polygenic, and include breast cancer that we study here. According to the Centers for Disease Control (CDC), in the USA, breast cancer is considered to be the second most common form of cancer amongst women, [4], that in 2019 was forecast to 268,600 cases and 42,260 deaths in 2019. Here we advance new methodology to probe variation in expression of a group (network) of genes that may lead to disease. Understanding the gene interaction network structure may be crucial to the development of future treatments. However, the inference of the underlying network structure of the interacting genes from gene expression data is a current and challenging problem. Network inference itself has many applications beyond cancer research, including fMRI network inference [5], drug-target interaction networks [6], and earthquake network inference [7] and economy issues [8] to name a few.

Many attempts to infer network structure from multivariate temporal data sets include Granger causality [9], for linear stochastic processes as well as transfer entropy (TE) [10] based on information theory for nonlinear processes. When

applied to a system of more than two factors, both of these concepts are unable to distinguish direct versus indirect effects and therefore systematically yield many false positive connections. To this end, we developed causation entropy (CSE) as a generalization of transfer entropy [11, 12], that compute the information flow between two factors, conditioned on a tertiary intermediary factors. In past studies, TE as well as CSE were computed nonparametrically, in terms of the mutual information estimator of Kraskov-Stögbauer-Grassberger (KSG) [13] using K-nearest neighbors (KNN) and from there we could invoke the oCSE greedy search algorithm [12] to deduce the complete network. However, specific knowledge of the joint distribution of the interacting variables lead to considerable computation efficiencies, such as the CSE computation based on jointly Gaussian variables [12] or jointly Laplace distributed variables in [14].

Some real world data, including gene expression data, is discretely distributed as a time-point process (TPP) rather than continuous valued in nature. Such data is often either jointly Poisson distributed or at least nearly Poisson in nature. While TPP are relatively common, as far as we know, no efficient joint entropy estimator exists. To this end, the main goal of this paper is to fill that void. This paper is structured as follows: we first provide a brief introduction to the mathematical background including the multivariate Poisson model we have chosen to work with and the various information theoretic quantities which are necessary in the oCSE method. Next we discuss our methods, including how we estimate the joint entropy in the case of Poisson variables, which allows us to calculate the various mutual informations, and then how we estimate network structure using these quantities. Finally, in the Results section we show how our method outperforms

---

\* fishja@clarkson.edu

both the nonparametric KNN version of oCSE and perhaps more surprisingly, our method outperforms the Gaussian estimator in a wide variety of contexts, and we apply our method to a breast cancer data set.

The main premise of this paper is to develop a computationally efficient approach to estimate joint entropy and related information theoretic measures for discrete-valued data, where the data often contains a significant fraction of zeros. Such data is commonly seen in systems biology, for example gene expression datasets. The main challenge comes from the discrete and multivariate nature of the data. We model discrete-valued multivariate data as a multivariate Poisson distribution, whose entire PDF can be completely specified by estimating the covariance parameters of the empirical distribution. From the Poisson model, we derive analytical expression of joint entropy and mutual information which come out as infinite series. To make them practical, we further develop truncated, finite-sum versions of the Poisson joint entropy, which can be used as building blocks for the approximate estimation of other important measures such as mutual information, transfer entropy and causation entropy.

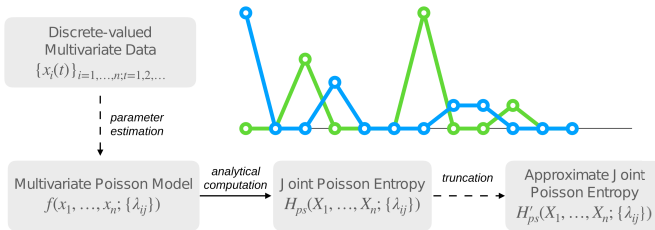


Figure 1. We develop a computationally efficient approach to estimating the joint entropy of Poisson distributed variables. We begin by assuming a multivariate Poisson model, we then estimate the parameters for this model from a multivariate discrete valued dataset and finally calculate the joint entropies using an approximation to the joint entropy.

## II. BACKGROUND

### A. Multivariate Poisson Model

First let us recall the single variate Poisson Model, which will be instructive in later sections [15]:

$$p(k) = \frac{\lambda^k}{k!} e^{-\lambda}. \quad (1)$$

The Poisson model has a multivariate generalization as follows, [16]:

$$P(X_1 = x_1, \dots, X_n = x_n) = \quad (2)$$

$$e^{-\sum_{i=1}^n \sum_{j \geq i} \lambda_{ij}} \sum_c \frac{\prod_{i=1}^n \lambda_{ii}^{(x_i - \sum_j a_{ij})} \prod_{i=1}^n \prod_{j > i} \lambda_{ij}^{a_{ij}}}{\prod_{i=1}^n (x_i - \sum_j a_{ij})! \prod_{i=1}^n \prod_{j > i} a_{ij}!},$$

where the set

$$\mathcal{C} = \quad (3)$$

$$\{A = [a_{ij}]_{n \times n} | a_{ij} \in \mathbb{N}_0, a_{ii} = 0, a_{ij} = a_{ji} \geq 0, \sum_j a_{ij} \leq x_i\},$$

and  $\mathbb{N}_0 = \mathbb{N} \cup \{0\}$ . This model is based on assuming that the  $x_i$  are linearly transformed from a set of independently drawn Poisson variables. We begin with

$$X \in \mathbb{N}_0^{n \times t} = (x_1, x_2, \dots, x_n)^T = BY, \quad (4)$$

$$Y \in \mathbb{N}_0^{m \times t} = (y_{11}, y_{22}, \dots, y_{nn}, y_{12}, y_{13}, \dots, y_{(n-1)n})^T.$$

Here each  $y_{ij}$  is independent Poisson, that is:  $y_{ij} \in \mathbb{N}_0^t \sim \text{Poisson}(\lambda_{ij})$ , (for  $i = 1, \dots, n, j \geq i$ ), so  $m = n + \frac{n(n-1)}{2}$ ,  $B \in \mathbb{N}_0^{n \times m}$ . Note that in this case  $\lambda_{ij} = \lambda_{ji}$ . The rows of  $X$  thus represent Poisson random variables which have  $t$  observations. Although the number of parameters needed to specify this model grows quickly, there are some nice properties. For instance, this model allows a simple estimate of each  $\lambda_{ij}$  since the sum of independent Poisson variables yields the following covariance matrix structure:

$$\text{Cov}(X) = \begin{bmatrix} \lambda_{11} + \sum_{j \neq 1}^n \lambda_{1j} & \lambda_{12} & \dots & \lambda_{1n} \\ \lambda_{12} & \lambda_{22} + \sum_{j \neq 2}^n \dots & & \lambda_{2n} \\ \vdots & \vdots & \dots & \vdots \\ \lambda_{n1} & \lambda_{n2} & \dots & \lambda_{nn} + \sum_{j=1}^{n-1} \lambda_{nj} \end{bmatrix} \quad (5)$$

with  $\lambda_{ij} = \lambda_{ji}$ . Here the  $(i, j)$  entries of the covariance matrix represent  $\text{cov}(x_i, x_j)$ , where  $\text{cov}(\cdot, \cdot)$  is the covariance between the two random variables. Proof of Eq. 43 may be found in the appendix.

This model has the advantage of extending the Poisson model to incorporate multiple variables that are not necessarily independent. However, there are also several limitations to this model. Those of primary interest to the current work we will now list. One limitation is the rapid growth in the number of states and parameters with respect to the number of variables, making calculation of the joint distribution computationally expensive. Another limitation is the model does not allow for negative covariance [16]. These difficulties are particularly complicating in the forth coming entropy computations and thus will be handled in later sections.

## B. Transfer Entropy and Causation Entropy

We will briefly review the various types of Shannon entropies, building toward the concepts of transfer entropy and causation entropy. These are the fundamental concepts of information flow we use to consider network inference. The Shannon *entropy* of a (discrete) random variable  $X$  is given by [18, 19]:

$$H(X) = - \sum_{x \in X} P(x) \log(P(x)), \quad (6)$$

where  $P(x)$  is the probability that  $X = x$  and we define  $0 \log(0) = 0$ . For the remainder of this paper we choose the natural log and thus all entropies will be measured in nats. Entropy can be thought of as a measure of how uncertain we are about a particular outcome. As an example we can imagine two scenarios, in one case we have a random variable  $X_1 = (x_1^{(1)}, x_1^{(2)}, \dots, x_1^{(n)})$  with  $x_1^{(t)} = 0 (\forall t)$ , that is  $P(X_1 = 0) = 1$ , in the other case the random variable  $X_2 = (x_2^{(1)}, x_2^{(2)}, \dots, x_2^{(n)})$  with  $P(X_2 = 0) = 0.5$ ,  $P(X_2 = 1) = 0.5$ . Here  $H(X_1) = 0$  nats, while  $H(X_2) = \ln(0.5)$  nats which happens to be the maximum for this case [19]. Thus it is easy to see that Shannon entropy reaches its greatest value when we are the most uncertain about the outcome, and its minimal value (0) when we are completely certain about the outcome. We can now examine the case of two random variables  $X$  and  $Y$ . In this case we may define the (discrete) *joint entropy* as [19]:

$$H(X, Y) = - \sum_{X=x} \sum_{Y=y} P(x, y) \ln(P(x, y)). \quad (7)$$

When the two random variables  $X$  and  $Y$  are independent  $H(X, Y) = H(X) + H(Y)$  which is the maximum joint entropy. Thus  $H(X, Y) \leq H(X) + H(Y)$ . The concepts of entropy and joint entropy may be extended to continuous variables by replacing the summations with integrals. We may also define the *conditional entropy* as:

$$H(X|Y) = - \sum_{x \in X} \sum_{y \in Y} P(x, y) \ln P(x|y). \quad (8)$$

The conditional entropy gives us a way to determine the relationship between variables, which is the key to network inference. If knowledge of the variable  $Y$  gives us complete knowledge of the variable  $X$  then the conditional entropy will be  $H(X|Y) = 0$  nats. Another important Shannon entropy is the *mutual information* which is defined as [19]:

$$\begin{aligned} I(X, Y) &= \sum_{x \in X} \sum_{y \in Y} P(x, y) \ln \left( \frac{P(x, y)}{P(x)P(y)} \right) = \\ &= H(X) - H(X|Y) = \\ &= H(X) + H(Y) - H(X, Y). \end{aligned} \quad (9)$$

We will now define the *Kullback-Leibler (KL) divergence* ( $D_{KL}$ ) [19]:

$$D_{KL}(P||Q) = - \sum_{x \in X} P(x) \ln \left( \frac{Q(x)}{P(x)} \right). \quad (10)$$

The KL divergence may be thought of as a measure of the distance between two distributions, though it is not a metric as it does not satisfy symmetry (that is in general  $D_{KL}(P||Q) \neq D_{KL}(Q||P)$ ), it also does not satisfy the triangle inequality. We can thus rewrite Eq. 9 in terms of KL divergence as [19]:

$$I(X, Y) = D_{KL}(P(x, y)||P(x)P(y)). \quad (11)$$

For a stationary stochastic process  $\{X^t\}$  the *entropy rate* is defined as [11]:

$$H(\chi) = \lim_{t \rightarrow \infty} H(X^t | X^{t-1}, X^{t-2}, \dots, X^1). \quad (12)$$

If the process is Markov (that is the process only depends upon its previous state and not states before that) then [19]:

$$H(\chi) = \lim_{t \rightarrow \infty} H(X^t | X^{t-1}). \quad (13)$$

The *transfer entropy* from  $X_2$  to  $X_1$  may be defined as [10, 11]:

$$T_{X_2 \rightarrow X_1} = H(X_1^{t+1} | X_1^t) - H(X_1^{t+1} | X_1^t, X_2^t). \quad (14)$$

*Causation entropy* is then a generalization of the transfer entropy, where [11, 12]:

$$C_{\mathcal{Q} \rightarrow \mathcal{P} | \mathcal{S}} = H(\mathcal{P}^{t+1} | \mathcal{S}^t) - H(\mathcal{P}^{t+1} | \mathcal{S}^t, \mathcal{Q}^t). \quad (15)$$

In Eq. 15  $\mathcal{P}, \mathcal{Q}$  are stochastic, Markov processes and  $\mathcal{S}$  are

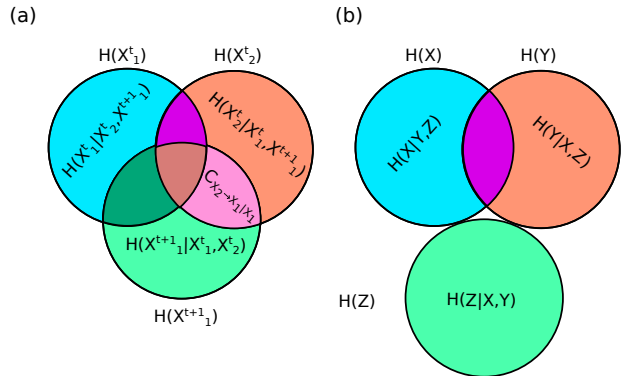


Figure 2. (a) The causation entropy between  $X_2$  and  $X_1$  is shown. In this case since we are only conditioning on  $X_1^t$ ,  $C_{X_2 \rightarrow X_1 | X_1^t} = T_{X_2 \rightarrow X_1}$ . Of course  $X_1^{t+1}$  may be replaced with a set of variables. (b) Here we show a special case where  $Z$  is independent of both  $X$  and  $Y$ . In this case it becomes clear that  $H(Z|X, Y) = H(Z)$ ,  $H(X|Y, Z) = H(X|Y)$  and  $H(Y|X, Z) = H(Y|X)$ . As explained in the text, this special case helps us to discern what are the proper variables to use in the Poisson case.

sets of stochastic Markov processes. Thus causation entropy allows us to determine if a process is influencing another process after conditioning out the influence of other processes. An example of causation entropy is shown in Fig. 2 (a). In theory if a process  $X$  has no influence over another process  $Y$ , the causation entropy after conditioning out the remaining processes would be identically 0, allowing us to reject a connection between  $X$  and  $Y$ . In practice however, due to

finite sampling this will not be identically 0. Further complicating this is the computational complexity for comparing every possible pair of nodes and then every triplet and quadruplet and so on becomes large for and increasing number ( $n$ ) of processes. This led to the development of an algorithm, referred to as optimal causation entropy (oCSE) [12]. In oCSE the finite sample size problem may be solved numerically by completing a statistical significance test in which a number ( $n_{shuffles}$ ) of random time shuffles of the data and determining if the causation entropy of unshuffled case is larger than a certain percentage ( $\theta \in [0, 1]$ ) of the shuffled cases. The issue of computational complexity is resolved by a two step algorithm. The first step is an aggregative discovery step, in which the node ( $j$ ) with maximal causation entropy to node  $i$  (if it is determined to be statistically significant) is added to the set of influencers  $\mathcal{K}$ , which is followed by the node  $k$  with maximal causation entropy after conditioning out node  $j$  and so on until no nodes have a statistically significant contribution. The second step is a removal step, where nodes  $l$  are removed from the set  $\mathcal{K}$  that is  $\hat{\mathcal{K}} = \mathcal{K} - l$  and if the causation entropy is determined to be 0 on this reduced set then  $\mathcal{K} \rightarrow \hat{\mathcal{K}}$  [12]. In some cases the information flow that we are interested in may be instantaneous, or at least effectively instantaneous, in which case introducing a time shift becomes unnecessary. In such situations a similar algorithm can be utilized, which is called optimal Mutual Information Interaction (oMII) [14]. We note here that since the Poisson model presented in Eqs. 2, 3, 4 has an instantaneous interaction among the variables, the oMII approach is more appropriate, and thus is the approach which will be presented for the remainder of this paper.

### III. ENTROPY ESTIMATION FROM MULTIVARIATE POISSON DATA

#### A. Estimating Joint Entropy of Poisson Systems

As was shown in the previous section, estimation of causation entropy requires calculation of conditional entropies,

which in turn can be computed from the joint entropy. However Eq. 2 does not yield an analytical solution for the calculation of the joint entropy. In fact, there is no analytical solution for even the simplest case (Eq. 1), forcing us to estimate the entropy from joint probabilities. As discussed above, it is computationally expensive to estimate the joint probabilities of the multivariate system. Estimation of the joint entropy becomes computationally expensive as a result, hampering the ability to calculate the causation entropy. To avoid this problem we present an approximation which allows us to obtain a computationally efficient estimate of the joint entropy.

#### B. Poisson Entropy

We begin by showing the Poisson Entropy:

$$H_{Poisson}(K) = - \sum_{k=0}^{\infty} \frac{\lambda^k}{k!} e^{-\lambda} \ln\left(\frac{\lambda^k}{k!} e^{-\lambda}\right) = \quad (16)$$

$$- \sum_{k=0}^{\infty} \frac{\lambda^k}{k!} e^{-\lambda} [-\lambda + k \ln(\lambda) - \ln(k!)] =$$

$$\lambda - \lambda \ln(\lambda) + \sum_{k=0}^{\infty} \frac{\lambda^k}{k!} e^{-\lambda} \ln(k!).$$

Thus the Poisson entropy does not have a finite term analytical expression, however the entropy can be estimated to within machine precision by truncating at a large value of  $k$ , and in this case it can be done with low computation time.

#### C. Bivariate Poisson Entropy

The Bivariate Poisson case is instructive to the n-variate Poisson case and therefore is presented now. The Bivariate Poisson can be rewritten as:

$$P(x_1, x_2) = e^{-\lambda_{11} - \lambda_{22} - \lambda_{12}} \frac{\lambda_{11}^{x_1}}{x_1!} \frac{\lambda_{22}^{x_2}}{x_2!} \left( \sum_{a_{12}=0}^{\min(x_1, x_2)} \frac{x_1!}{(x_1 - a_{12})!} \frac{x_2!}{(x_2 - a_{12})!} \frac{a_{12}!}{a_{12}!} \left( \frac{\lambda_{12}}{\lambda_{11} \lambda_{22}} \right)^{a_{12}} \right). \quad (17)$$

We will let  $d_{12} = \frac{\lambda_{12}}{\lambda_{11} \lambda_{22}}$  and  $D(x_1, x_2) = \sum_{a_{12}=0}^{\min(x_1, x_2)} \frac{x_1!}{(x_1 - a_{12})!} \frac{x_2!}{(x_2 - a_{12})!} \frac{d_{12}^{a_{12}}}{a_{12}!}$ . Then Eq. 17 will become:

$$P(x_1, x_2) = e^{-\lambda_{11} - \lambda_{22} - \lambda_{12}} \frac{\lambda_{11}^{x_1}}{x_1!} \frac{\lambda_{22}^{x_2}}{x_2!} D(x_1, x_2). \quad (18)$$

Now to get the joint entropy of the Bivariate Poisson we have:

$$H(X_1, X_2) = - \sum_{x_1=0}^{\infty} \sum_{x_2=0}^{\infty} P(x_1, x_2) \ln(P(x_1, x_2)) = - \sum_{x_1=0}^{\infty} \sum_{x_2=0}^{\infty} \quad (19)$$

$$e^{-\lambda_{11}-\lambda_{22}-\lambda_{12}} \frac{\lambda_{11}^{x_1}}{x_1!} \frac{\lambda_{22}^{x_2}}{x_2!} D(x_1, x_2) [-\lambda_{11} - \lambda_{22} - \lambda_{12} + x_1 \ln(\lambda_{11}) + x_2 \ln(\lambda_{22}) - \ln(x_1!) - \ln(x_2!) + \ln(D(x_1, x_2))]. \quad (20)$$

A scenario of interest arises when  $\lambda_{11}, \lambda_{22}$ , and  $\lambda_{12}$  are all small and  $\lambda_{12} \ll \lambda_{11}\lambda_{22}$ . In this case we have  $D(x_1, x_2) \approx \sum_{a_{12}=0}^{\min(x_1, x_2)} \frac{d_{12}^{a_{12}}}{a_{12}!}$ , since the  $d_{12}$  term dominates in this case. Note we require  $\lambda_{11}$  and  $\lambda_{22}$  to be small to ensure that the large  $x_1$  and  $x_2$  terms to become insignificant in Eq. 20. Thus we have  $D(x_1, x_2) \approx 1 + \frac{d_{12}^2}{2!} + \dots \approx 1$ . Now by grouping the terms and remembering (the middle part of) Eq. 16, plugging in  $D(x_1, x_2) = 1$  and taking the infinite sums, we can see that Eq. 20 can be written:

$$H(X_1, X_2) = e^{-\lambda_{12}} [H(X_1) + H(X_2) + \lambda_{12}]. \quad (21)$$

Remembering that we assumed  $\lambda_{12} \ll 1$  we can further reduce Eq. 22 to:

$$H(X_1, X_2) = [H(X_1) + H(X_2) + \lambda_{12}]. \quad (22)$$

As Fig. 3 shows, this approximation works well when  $d_{12} \ll 1 \implies \lambda_{12} \ll \lambda_{11}\lambda_{22}$ , and in this regime the error will be small. Similar analysis can be carried out for the larger multivariate cases which allows us to arrive at a general formula for our approximation given by:

$$H(X_1, X_2, \dots, X_n) \approx [H(X_1) + H(X_2) + \dots + H(X_n) + \sum_{j>i} \lambda_{ij}], \quad (23)$$

where we are assuming that  $\lambda_{ij}$  are small for all  $(i, j)$  pairs. Fortunately as we can see in Eq. 23, all of the quantities on the right hand side are computationally efficient to compute. This in fact greatly reduces the computational time necessary for estimation of the joint entropy.

A note on the entropy calculations is required here however. When calculating the mutual information in the Poisson model, care must be taken because of how the marginals of a joint Poisson process are drawn. For example from Eq. 9 it may be tempting to say that:

$$I_{\text{Poisson}}(X_1, X_2) = H(X_1) + H(X_2) - H(X_1, X_2), \quad (24)$$

with  $X_1 \sim \text{Poisson}(\lambda_{11})$  and  $X_2 \sim \text{Poisson}(\lambda_{22})$ . However this is not exactly correct, though the error here is subtle. In fact we must make a small change to Eq. 24 to be:

$$I_{\text{Poisson}}(X_1, X_2) = H(\hat{X}_1) + H(\hat{X}_2) - H(X_1, X_2), \quad (25)$$

here  $X_1 \sim \text{Poisson}(\lambda_{11})$  and  $X_2 \sim \text{Poisson}(\lambda_{22})$ , but  $\hat{X}_1 \sim \text{Poisson}(\lambda_{11} + \lambda_{12})$  and  $\hat{X}_2 \sim \text{Poisson}(\lambda_{22} + \lambda_{12})$ . This subtle difference is important, because without recognizing this fact, the calculated mutual information becomes negative, which violates our well established condition that mutual information be positive. The need for  $\hat{X}_1$  and  $\hat{X}_2$  is apparent from Eq. 43, when two Poisson random variables are summed together their *marginals* then are drawn from the sum of the underlying rate (i.e.  $\lambda_{ii}$ ) and the coupling rate (i.e.  $\lambda_{ij}$ ). This also transfers to computing the conditional mutual information. To better illuminate this calculation it is helpful to refer to Fig. 2 (b).

$$I(X, Y|Z) = H(X, Z) + H(Y, Z) - H(X, Y, Z) - H(Z). \quad (26)$$

In the special case presented in Fig. 2 (b) Eq. 35 becomes

$$I(X, Y|Z) = I(X, Y) = H(X) + H(Y) - H(X, Y), \quad (27)$$

and thus

$$H(X) + H(Y) - H(X, Y) = H(X, Z) + H(Y, Z) - H(X, Y, Z) - H(Z). \quad (28)$$

In this special case we can note the following:

$$H(Y, Z) = H(Y) + H(Z). \quad (29)$$

Applying Eq. 29 to Eq. 28 we find that:

$$H(X) - H(X, Y) = H(X, Z) - H(X, Y, Z). \quad (30)$$

We know from Eq. 25 that in the Poisson case this becomes:

$$H(\hat{X}) - H(X, Y) = H(X, Z) - H(X, Y, Z). \quad (31)$$

Applying the following facts to Eq. 31

$$\begin{cases} H(X, Y, Z) = H(X, Y) + H(Z), \\ \text{and } H(X, Z) = H(X) + H(Z), \end{cases} \quad (32)$$

we find that:

$$H(\hat{X}) = H(X). \quad (33)$$

Similar analysis also shows that:

$$H(\hat{Y}) = H(Y), \quad (34)$$

this implies that we must use the Poisson marginals in the computation of the conditional mutual information. That is in the Poisson case we must have:

$$I(X, Y | Z) = H(\hat{X}, Z) + H(\hat{Y}, Z) - H(X, Y, Z) - H(Z). \quad (35)$$

Note the use of  $\hat{X}$  and  $\hat{Y}$  in this case. This distinction in the Poisson case is important because we note that without using the proper marginals the computation results in *negative* conditional mutual information which is clearly not correct since conditional mutual information must be positive [19].

Importantly the new definition given in Eq. 23 becomes more computationally efficient than computing the Poisson joint entropy directly from the joint probability. This requires calculation of only separate *single* variate entropies which is requires less computation. This naturally leads to the question of the accuracy of this new model. As can be seen in Fig. 4 the new definition of entropy still leads to accurate identification of network structure. This new definition also fits into the general framework of entropy which was developed above, allowing us to apply the oMII algorithm to the data.

#### D. Estimating Network Structure

Often the interaction of different agents is what guides the overall behavior of a system, and thus it is necessary to know which agents are interacting. In a gene interaction network this may be crucial to understanding how future treatments could be developed, especially in the cases where more than a single gene may need to be targeted for therapy. Typically we have data but no knowledge of the underlying network structure *a priori*, therefore it becomes necessary to estimate the network structure from the data. Causation entropy allows us to accomplish this task as will be discussed below. We will begin by discussing graphs: A graph  $\mathcal{G}$  is a set of vertices  $\mathcal{V} \subset \mathbb{N}$  and edges  $\mathcal{E} \subset \mathcal{V} \times \mathcal{V}$ , that is:

$$\mathcal{G} = \{\mathcal{V}, \mathcal{E}\}. \quad (36)$$

We note that  $|\mathcal{V}| = n$  signifies that there are  $n$  vertices (or nodes) in  $\mathcal{G}$ , where  $|\cdot|$  denotes the cardinality of a set. The

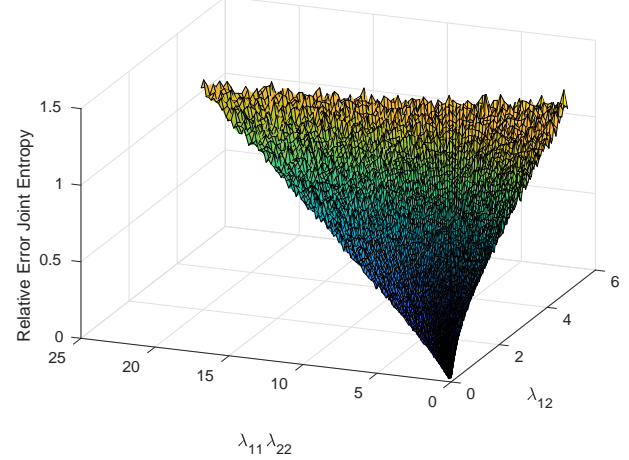


Figure 3. The relative error in the joint entropy calculation between the joint entropy calculated through truncation and the joint entropy calculated by our approximation. It is clear that when both  $\lambda_{12}$  and  $\lambda_{11}\lambda_{22}$  are small, the relative error is small. Thus we expect this approximation to work well when all of the estimated rates are small. In practice we find that when scaling the rates to be in  $[0, 1]$  we get good results, regardless of how high the true rates were.

adjacency matrix  $\mathcal{A} \in \mathbb{N}_0^{n \times n}$  is a matrix which encodes the graph structure, with

$$\begin{cases} \mathcal{A}_{ij} = 1 \text{ if } (i, j) \in \mathcal{E}, \\ \mathcal{A}_{ij} = 0 \text{ otherwise.} \end{cases} \quad (37)$$

When a system has a graph structure it is often referred to as a network. The adjacency matrix then encodes the network structure of the system. Our goal will be to get an estimated network structure  $\hat{\mathcal{A}}$  which is as close to possible to the real network structure, that is we want:

$$\|\mathcal{A} - \hat{\mathcal{A}}\|_0 \quad (38)$$

to be as small as possible (ideally 0). We would also like for this to be accomplished with as little data ( $t$ ) as possible, since we are often limited in the amount of real world data we receive. Our estimation of the network structure relies on nodes sharing information with one another. Thus  $\hat{\mathcal{A}}$  may be thought of as which nodes are directly communicating with one another, rather than strictly being the physical structure. However as has been seen in previous work [11, 12] and as we will see below the physical network structure and the information network structure align accurately in most situations.

#### E. Estimating Network Structure with Poisson

As we saw in a previous section, we can get a quick estimate of the Poisson entropy (and causation entropy). In this section we will utilize that estimate in order to estimate the underlying network structure of simulated data. The data is simulated using the multivariate Poisson model found in Eqs.

2 - 4. This model can be rewritten so as to incorporate the adjacency matrix  $\mathcal{A}$  and noise  $E$  as shown in [20, 21] as:

$$X = BY + E, \quad (39)$$

$$B = [I_n; P \odot (1_n tri(\mathcal{A})^T)] \quad (40)$$

where  $I_n$  is the  $(n \times n)$  identity matrix,  $P \in \mathbb{N}_0^{n \times (m-n)}$  is a permutation matrix with exactly  $n$  ones per row,  $\odot$  represents the Hadamard product,  $1_n \in \mathbb{N}^{n \times 1}$  is the vector of all ones,  $tri(\mathcal{A}) \in \mathbb{N}_0^{\frac{n(n-1)}{2} \times 1}$  denotes the vectorized upper triangular portion of the adjacency matrix, and  $E \in \mathbb{N}_0^{n \times t}$ . We have established in previous discussion that there is no analytical solution for the entropy of the multivariate Poisson, instead an approximation has been made. However since a Poisson distribution can be approximated by a Gaussian, it seems reasonable that the Poisson entropy could likewise be approximated by Gaussian entropy which does have an analytical solution. We show in Fig. 4 using the Gaussian version of the oCSE does well finding the true edges with a high true positive rate (TPR). The Gaussian oCSE finds the edges at the expense of a much larger false positive rate (FPR), however. We define TPR and FPR as follows: let  $\mathcal{G} = \{\mathcal{V}, \mathcal{E}\}$  be the true network structure and  $\hat{\mathcal{G}} = \{\hat{\mathcal{V}}, \hat{\mathcal{E}}\}$  be the estimated network structure, then:

$$TPR = \frac{|\mathcal{E} \cap \hat{\mathcal{E}}|}{|\mathcal{E}|}, \quad (41)$$

and

$$FPR = \frac{|\hat{\mathcal{E}} \setminus \mathcal{E}|}{|\mathcal{E}|}. \quad (42)$$

In this case  $\setminus$  represents set subtraction. Note that from this definition  $0 \leq TPR \leq 1$  while  $FPR \geq 0$ .

#### IV. RESULTS

The Poisson oMII method is tested on data simulated as described above. In Fig. 4 each data point is averaged over 50 realizations of the network dynamics. Two different Erdős-Rényi (ER) graph types are used, one with  $p = 0.04$  and one with  $p = 0.1$ . The parameter  $p$  in an ER graph controls the sparsity of the graph, thus the graphs with  $p = 0.1$  will have considerably more edges on average than graphs with  $p = 0.04$ . For these simulations  $n = 50$  was chosen. The rates were chosen to be  $\lambda_{ij} = 1$  ( $\forall i, j$ ) and  $E_i \sim \text{Poisson}(0.5)$  ( $\forall i$ ) where  $E_i \in \mathbb{N}_0^{t \times 1}$  are the columns of  $E$ . This is the high SNR scenario from [20]. To estimate the rates, we simply use a the MATLAB function corr. We note that corr does not determine the covariance matrix but rather the correlation matrix. The correlation guarantees the calculated rates will be relatively small and allows us to stay in the small relative error regime shown in Fig. 3. The correlation matrix then gives us all of the off diagonal rates  $\lambda_{ij}$  ( $i \neq j$ ) and to obtain the rates  $\lambda_{ij}$  ( $i = j$ ) we can see from Eq. 43

that we simply need to subtract the sum of the non-diagonal elements from the diagonal elements. That is if we let

$$\text{Corr}(X) = \begin{bmatrix} e_{11} & \lambda_{12} & \cdots & \lambda_{1n} \\ \lambda_{12} & e_{22} & \cdots & \lambda_{2n} \\ \vdots & \vdots & \cdots & \vdots \\ \lambda_{n1} & \lambda_{n2} & \cdots & e_{nn} \end{bmatrix}, \quad (43)$$

then  $\lambda_{ii} = e_{ii} - \sum_{j \neq i} \lambda_{ij}$ .

For testing on real world data, we run the Poisson oMII method on count data from breast cancer patients who have been screened for different micro RNA's (miRNA's). The data set is retrieved from the <https://portal.gdc.cancer.gov> website. Specifically the TCGA-BRCA raw sequencing miRNA data is used. In this case  $t = 1207$  and  $n = 1881$  different miRNA's. Of these 1881 miRNA's  $\approx 1000$  pass the two sample Kolmogorov-Smirnov (KS) [25] test as being Poisson (in this case a comparison sample of length 10000 samples is drawn to compare with the data from a Poisson distribution), with the KS level  $\alpha = 0.05$ . The remaining  $\approx 900$  miRNA data were then scaled as follows:

$$x_i^* \in \mathbb{N}_0^{1207 \times 1} = \lfloor \frac{x_i}{\langle x_i \rangle} \rfloor. \quad (44)$$

In this case  $\langle \cdot \rangle$  represents the mean and  $\lfloor \cdot \rfloor$  represents the floor function which is utilized to convert the newly scaled data back to integer data. The floor function being applied to the vector here simply means that the floor function was applied for each entry of the vector. After scaling the majority of the data appear to fit well (again determined by applying the KS test) to a negative binomial distribution with only  $\approx 200$  failing as both Poisson and negative binomial. We note here that the Poisson distribution is a special case of the negative binomial distribution. To see this it is useful to view the distribution as we do below:

$$P_{NegBin}(k) = \binom{k+r-1}{k} \lambda^k (1-\lambda)^r. \quad (45)$$

If we let  $r \rightarrow \infty$  in Eq. 45 it is easy to see that the term  $(1-\lambda)^r \rightarrow e^{-\lambda}$ , and rewriting  $\binom{k+r-1}{k} = \frac{(k+r-1)!}{k!(r-1)!} \rightarrow \frac{1}{k!}$ . Combining these facts gives the Poisson distribution, thus as  $r \rightarrow \infty$  the negative binomial distribution becomes the Poisson distribution.

Given that the majority of the data is negative binomial (the Poisson data also can be fit as negative binomial) we must interpret the results of with caution especially in light of the results shown in Fig. 4. The results of the application of the Poisson oMII still are interesting, especially given that the negative binomial distribution can be viewed as a compound Poisson distribution [22, 23]. To obtain the networks shown in Fig. 5 we first restricted the data to having a minimum of 10 total counts, this was to avoid including data that had zero variation or near zero variation. This restriction left us with 1403 miRNA's, oMII was then run on the remaining data which resulted in the network shown in Fig. 5 (a). The network has many miRNA's which appear to be noninteracting, however there are several weakly connected components. When we

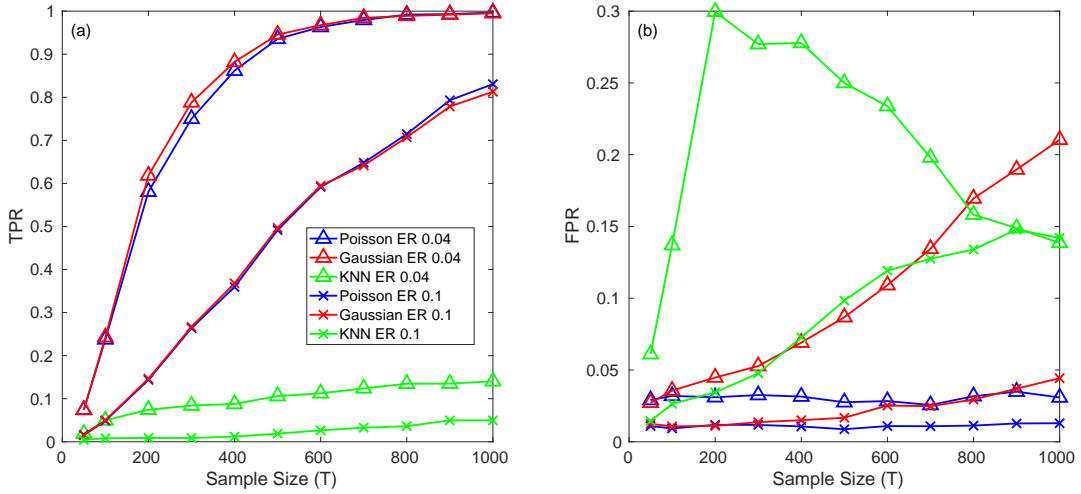


Figure 4. Two different types of Erdős-Rényi (ER) graphs were used as the underlying true network structure for the simulated data, the triangles represent 50 node ER graphs with  $p = 0.04$  and the x's represent 50 node ER graphs with  $p = 0.1$ . The blue lines represent the Poisson oMII, the red lines represent the Gaussian oMII, and the green lines represent the KNN oMII. In (a) the true positive rate (TPR) is shown for different sample sizes, each point is averaged over 50 realizations of the network dynamics. In (b) the false positive rate (FPR) is shown. As can be seen the Gaussian oMII performs as well as Poisson oMII in TPR with the KNN performing poorly, but the Poisson oMII significantly outperforms both the Gaussian and the KNN oMII in terms of FPR. With increasing data the Gaussian oMII tends to overestimate the number of edges. The nonparametric KNN method performs poorly on both TPR and FPR, generally the KNN method requires much more data for improved accuracy. However as the sample size increases so does the FPR of the KNN version of oMII.

focus on the largest weakly connected component, shown in Fig. 5 (b), we found that many miRNA's that have been previously identified as up or down regulated in breast cancer end up in this component, this component included most of the miRNA's listed in Table 1 of [24]. The up and down regulated miRNA's will be referred to as the interesting miRNA's for brevity.

We then decided to focus on this largest weakly connected component which contains 619 miRNA's. We decided to limit ourselves to the miRNA's which have a reasonable amount of counts (that is the ones which have counts for most of the patients included in the study) and thus we further restricted the data from the largest component to the miRNA's with at least 1000 counts. This reduced the miRNA's from 619 down to 226. We reran oMII on this reduced data set and we found on this set another group of weakly connected components. We note that it is not necessarily expected that these 226 miRNA's would be weakly connected since we removed a large number of miRNA's from the previous set. The largest component of this reduced set is shown in Fig. 5 (c) and contains 83 miRNA's. Several of the miRNA's in this component are interesting miRNA's. A feature that is clear in Fig. 5 (c) is the tripartite nature of the weakly connected component. It appears that this portion of the network is driven by a few miRNA's (shown at the top of Fig. 5). The four miRNA's with the highest out degree at the top of this net-

work are mir-1248, let-7a-2, mir-1179 and let-7b. All four of these are interesting miRNA's [24, 26–28] and they seem to be the main drivers, even of the other interesting miRNA's, for instance these miRNA's appear to be the drivers of some of the miRNA 200 family in the network and also drivers of the some of the let-7 family which are also interesting miRNA's [26, 29]. This suggests that it may be possible to target a small number of miRNA's for some desired behavior of the system of miRNA's in drug development.

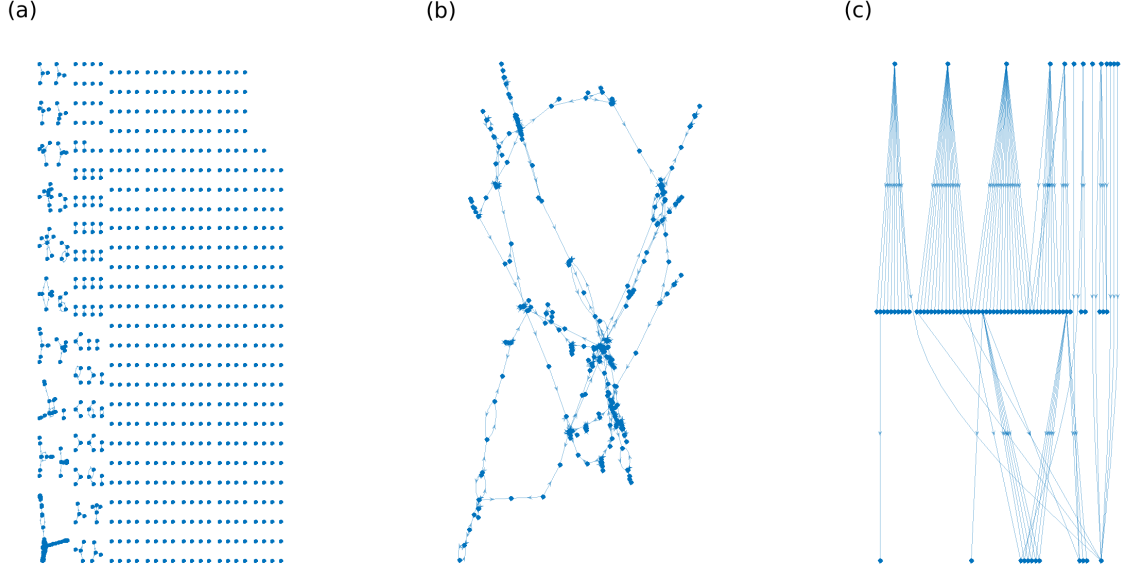


Figure 5. Example networks generated by the Poisson oMII algorithm. (a) The full network of the 1403 miRNA's with more than 10 total counts in the dataset. (b) The largest weakly connected component from (a) which contains 619 miRNA's. (c) After reducing the data as described in the text to 226 miRNA's this is the largest component of that network and contains 83 miRNA's. Note that the structure of (c) appears tripartite and the nodes at the top appear to be drivers of the network.

## V. CONCLUSION

In this paper we have given an approximation to the mutual information of a multivariate Poisson system. We have shown through numerical experiments that this approximation works efficiently, and the results of network estimation indicate that the approximation is justified. We have also developed the oMII (and by extension the oCSE) algorithm for computation of the causation entropy of a Poisson system based on the joint entropy approximation discussed above. We have shown that this model is superior to simply assuming the data is Gaussian, which is likely related to the strange behavior of the marginals in a Poisson system, as we have outlined above. The Poisson oMII algorithm also significantly outperforms the nonparametric KNN version of oMII. Finally, we have applied the Poisson oMII algorithm to a breast cancer miRNA expression count dataset, which has produced potentially interesting insights into the network of miRNA's as it relates to breast cancer. Our network inference on the breast cancer miRNA network has shown that there is a relationship between the highest variance (in expression values) of miRNA's. There seems to be unidirectional connections between these miRNA's, with certain miRNA's taking on the role of drivers in the network. This may suggest a future course of action for future drug development.

## VI. ACKNOWLEDGEMENTS

E.B. was supported by the Army Research Office (N68164-EG) and, J.F., E.B. and D.H. were supported by DARPA.

## VII. APPENDIX

Below we offer proof of Eq. 43.

*Proof.* Covariance of the multivariate Poisson

In the model presented in Eqs. 2, 3, 4, we can see that:

$$\begin{aligned}
 x_1 &= y_{11} + y_{12} + \dots + y_{1n} \\
 x_2 &= y_{12} + y_{22} + \dots + y_{2n} \\
 &\vdots \\
 x_n &= y_{1n} + y_{2n} + \dots + y_{nn}
 \end{aligned} \tag{46}$$

Without loss of generality we will look at the pair ( $i = 1, j = 2$ ). In this case we see that the covariance between this pair of random variables is defined:

$$\text{cov}(x_1, x_2) = \mathbb{E}[x_1 x_2] - \mathbb{E}[x_1] \mathbb{E}[x_2], \tag{47}$$

Considering Eqs. 46, 47 and noting  $y_{12} = y_{21}$ , we have:

$$\begin{aligned} \text{cov}(x_1, x_2) &= \mathbb{E} \left[ y_{12}^2 + \sum_{\substack{i=1 \\ i \neq 2}}^n \sum_{j=2}^n y_{1i} y_{2j} \right] \\ &\quad - \mathbb{E}[y_{11} + y_{12} + \dots + y_{1n}] \mathbb{E}[y_{12} + y_{22} + \dots + y_{2n}] \end{aligned} \quad (48)$$

Because the expectation is a linear operator, Eq. 48 can be

expressed as:

$$\begin{aligned} \text{cov}(x_1, x_2) &= E[y_{12}^2] + \mathbb{E} \left[ \sum_{\substack{i=1 \\ i \neq 2}}^n \sum_{j=2}^n y_{1i} y_{2j} \right] - \\ &\quad \left( \mathbb{E}[y_{12}] + \sum_{\substack{i=1 \\ i \neq 2}}^n \mathbb{E}[y_{1i}] \right) \left( \mathbb{E}[y_{12}] + \sum_{j=2}^n \mathbb{E}[y_{2j}] \right). \end{aligned} \quad (49)$$

From the independence of each  $y_{ij}$  the covariance can thus be expressed:

$$\begin{aligned} \text{cov}(x_1, x_2) &= \mathbb{E}[y_{12}^2] + \sum_{\substack{i=1 \\ i \neq 2}}^n \sum_{j=2}^n \mathbb{E}[y_{1i} y_{2j}] - \\ &\quad \mathbb{E}^2[y_{12}] - \sum_{\substack{i=1 \\ i \neq 2}}^n \sum_{j=2}^n \mathbb{E}[y_{1i} y_{2j}] = \\ &\quad \mathbb{E}[y_{12}^2] - \mathbb{E}^2[y_{12}] = \\ &\quad \text{Var}(y_{12}). \end{aligned} \quad (50)$$

Since  $y_{12}$  is independent Poisson and from the variance of an independent Poisson random variable  $\text{Var}(y_{12}) = \lambda_{12}$ . Applying this to each  $i, j (i \neq j)$  pair gives the desired covariance structure.  $\square$

---

[1] C. S Rogers, et. al. **Disruption of the CFTR Gene Produces a Model of Cystic Fibrosis in Newborn Pigs** *Science* 321, 1837-1841 (2008)

[2] P. Sebastiani, M. F. Ramoni, V. Nolan, C. T. Baldwin, M. H. Steinberg **Genetic Dissection and Prognostic Modeling of Overt Stroke in Sickle Cell Anemia** *Nature Genetics* 37, 435 (2005)

[3] K. De Boulle, et. al. **A Point Mutation in the FMR-1 Gene Associated with Fragile-X Mental Retardation** *Nature Genetics* 3, 31 (1993)

[4] <https://www.cdc.gov/cancer/breast/statistics/index.htm> (2019)

[5] S. M. Smith **The Future of FMRI Connectivity** *Neuroimage* 62, 1257-1266 (2012)

[6] Y. Yamanishi, J. P. Vert, M. Kanehisa **Prediction of Drug-Target Interaction Networks from the Integration of Chemical and Genomic Spaces** *Bioinformatics* 21, i468-i477 (2008)

[7] Y. Zhang, H. Zhao, X. He, F. D. Pei, G. G. Li **Bayesian Prediction of Earthquake Network Based on Space-Time Influence Domain** *Physica A* 445, 138-149 (2016)

[8] G. Iori et. al **A network analysis of the Italian overnight money market** *Journal of Economic Dynamics and Control* 32, 259-278 (2008)

[9] C. W. Granger **Investigating Causal Relations by Econometric Models and Cross-Spectral Methods** *Econometrica: Journal of the Econometric Society* 424-438, (1969)

[10] T. Schreiber **Measuring Information Transfer** *Phys. Rev. Lett.* 85, 461 (2000)

[11] J. Sun, E. M. Bolt **Causation Entropy Identifies Indirect Influences, Dominance of Neighbors and Anticipatory Couplings** *Physica D* 267, 49 (2014)

[12] J. Sun, D. Taylor, E. M. Bolt **Causal Network Inference by Optimal Causation Entropy** *SIAM J. Appl. Dyn. Sys.* 14, 73 (2015)

[13] A. Kraskov, H. Stögbauer P. Grassberger **Estimating Mutual Information** *Physical Review E* 69, 066138 (2004)

[14] A. S. Ambgedara, J. Sun, K. Janoyan, E. M. Bolt **Information Theoretical Noninvasive Damage Detection in Bridge Structures** *Chaos* 26, 116312 (2016)

[15] E. M. Bolt, N. Santitissadeekorn **Applied and Computational Measurable Dynamics** *SIAM* 2013

[16] D. Karlis, L. Meligotsidou **Finite Mixtures of Multivariate Poisson Distributions with Application** *Journal of Statistical Planning and Inference* 137, 1942-1960 (2007)

[17] D. I. Inouye, E. Yang, G. I. Allen, P. Ravikumar **A Review of Multivariate Distributions for Count Data Derived from the Poisson Distribution** *Wiley Interdisciplinary Reviews: Comp. Statistics* 9, e1398 (2017)

[18] C. E. Shannon **A Mathematical Theory of Communication** *The Bell Systems Technical Journal* 27, 379-423 (1948)

[19] T. M. Cover, J. A. Thomas **Elements of Information Theory** *John Wiley & Sons* (2012)

[20] G. I. Allen, Z. Liu **A Local Poisson Graphical Model for Inferring Networks From Sequencing Data** *IEEE Trans NanoBiosci* 12, 189-198 (2013)

- [21] M. Gallopin, A. Rau, F. Jaffrézic **A Hierarchical Poisson Log-Normal Model for Network Inference from RNA Sequencing Data** *PloS One* 8, e77503 (2013)
- [22] F. J. Anscombe **Sampling Theory of the Negative Binomial and Logarithmic Series Distributions** *Biometrika* 37, 358-382 (1950)
- [23] A. F. Bissell **A Negative Binomial Model with Varying Element Sizes** *Biometrika* 59, 435-441 (1972)
- [24] M. V. Iorio, M. Ferracin, C. Liu, A. Veronese, et. al. **MicroRNA Gene Expression Deregulation in Human Breast Cancer** *Cancer Research* 65, 7065-7070 (2005)
- [25] H. W. Lilliefors **On the Kolmogorov-Smirnov Tst for Normality with Mean and Variance Unknown** *Journal of the American Statistical Association* 62, 399-402 (1967)
- [26] C. K. Thammaiah, S. Jayaram **Role of let-7 Family MicroRNA in Breast Cancer** *Non-coding RNA research* 1, 77-82 (2016)
- [27] I. Medimegh, W. Troudi, N. Stambouli et. al. **Wild-Type Genotypes of BRCA1 Gene SNPs Combined with MicroRNA Over-Expression in Mammary Tissue Leading to Familial Breast Cancer with an Increased Risk of Distant Metastases' Occurrence** *Medical Oncology* 31, 255 (2014)
- [28] M. Tanic, K. Yanowski, G. Gómez-López et. al. **MicroRNA Expression Signatures for the Prediction of BRCA1/2 Mutation-Associated Hereditary Breast Cancer in Paraffin-Embedded Formalin-Fixed Breast Tumors** *International Journal of Cancer* 136, 593-602 (2015)
- [29] P. A. Gregory, A. G. Bert, E. L. Paterson et. al. **The MiR-200 Family and MiR-205 Regulate Epithelial to Mesenchymal Transition by Targeting ZEB1 and SIP1** *Nature Cell Biology* 10, 593 (2008)